Conformation of Antamanide–Sodium in Solution†,‡

Dinshaw J. Patel

ABSTRACT: Proton and carbon nmr and model building studies were combined to generate conformations for antamanide–Na in solution. The N, H^{α}, and H^{β} proton chemical shifts were related by spin decoupling experiments. Temperature coefficient and exchange studies elucidated the nature of the exchangeable peptide N protons in the complex. Coupling constant and chemical-shift changes observed on complexation permitted identification of those residues undergoing conformational change. At low Na ion concentration, a study of metal ion exchange between antamanide and its complex suggested the absence of cis–trans peptide bond isomerization for antamanide on complexation. An analysis of the carbon chemical shifts suggests that the complex contains two cis and two trans X-Pro peptide bonds. Low-energy conformations for the complex containing a cavity for metal ion binding were generated with all-trans peptide bonds (*trans*-complex), cis peptide bonds at Val_1-Pro_2 and Phe_6-Pro_7 (1,6-*cis*-complex), and cis peptide bonds at Pro_2-Pro_3 and Pro_7-Pro_8 (2,7-*cis*-complex). These conformations were constructed from molecular model building after consideration of the nmr spectral parameters and conformational energy maps. The experimental evidence appears to be more consistent with conformation 1,6-*cis*-complex for antamanide–Na in solution. Addition of water to antamanide in nonaqueous solutions results in a conformational change without cis–trans peptide bond isomerization. A study of the temperature coefficients for the peptide N protons for the conformation of antamanide in aqueous media suggests similarities to the conformation of antamanide–Na in nonaqueous solvents.

In the previous manuscripts the solvent-dependent conformational characteristics of the cyclic decapeptide antamanide in nonaqueous solution were investigated using proton and carbon nuclear magnetic resonance (nmr), model building studies (Patel, 1973), and conformational calculations (Tonelli, 1973).

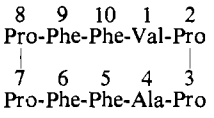

Antamanide forms stable complexes with monovalent Na and Tl and divalent Ca (Wieland *et al.*, 1972). Complex stability is strongly dependent on solvent polarity, with stability constants for Na ion in the range 30,000 (CD_3CN), 2000 (C_2H_5OH–H_2O (96:4)), and 0 (C_2H_5OH–H_2O (30:70)) (Wieland *et al.*, 1972).

Optical rotatory dispersion (ORD) and circular dichroism (CD) studies have demonstrated that antamanide in nonpolar solvents undergoes a conformational transformation on addition of water (Ivanov *et al.*, 1971; Faulstich *et al.*, 1972). Further, CD studies suggest that the antamanide conformation in aqueous media and the solvent-independent conformation of the antamanide–Na complex are similar (Faulstich *et al.*, 1972).

Using nmr, CD, and infrared (ir) spectroscopy, Ivanov *et al.* (1971) have proposed a conformation for the antamanide–Na complex in solution, designated *trans*-complex-M, in this study. The merits of this structure will be discussed later in this presentation.

This investigation reports on features of the conformation for antamanide in aqueous solution and the conformation of the sodium complex as derived from nmr and model building studies.

Experimental Section

Nmr spectra were run on a 220-MHz Varian spectrometer equipped with a Varian variable temperature unit. Ethylene glycol monitored temperatures to ±1°. A Fabri-Tek computer of average transients improved the signal-to-noise ratio. A Hewlett-Packard 651B test oscillator was used to carry out spin decoupling.

^{13}C nmr spectra were run on an XL-100 spectrometer interfaced with an F&H pulse programmer and a Fabri-Tek computer for operation in the Fourier transform mode (Sternlicht and Zuckerman, 1972). Proton decoupling was carried out under heteronoise conditions. Samples were dissolved in deuterated solvent and the instrument was locked on solvent deuterium.

Results and Discussion

As outlined in the previous manuscript (Patel, 1973), decoupling studies permit correlation of N, H^{α}, and H^{β} proton chemical shifts. The $J_{H^N H^{\alpha}}$ coupling constant limits the allowed values of the rotation angle φ, while the C^{β} and C^{γ} Pro carbon chemical shifts are a sensitive function of the configuration at the peptide bond. The temperature dependence of amide protons and their exchange properties are analyzed in terms of the hydrogen-bonded, buried, and solvent-exposed nature of the protons.

Antamanide–Sodium Complex in Solution

I. Nmr Spectral Parameters. The proton nmr spectrum of antamanide–Na (antamanide:NaSCN ≡ 1:1.75) in CD_3CN at 58° is shown in Figure 1. Decoupling studies permit the assignments shown below the spectra. The chemical shifts and coupling constants are summarized in Table I.

As noted earlier (Ivanov *et al.*, 1971), the six peptide NH

† From the Bell Laboratories, Murray Hill, New Jersey 07974. *Received July 24, 1972.*

‡ This paper and the previous paper both contain color plates. Plates 1–4 of this paper appear on p 685.

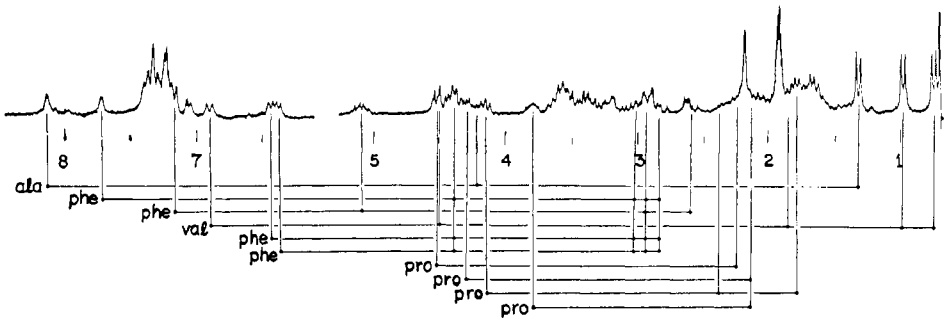

FIGURE 1: Proton nmr spectrum of antamanide-Na in CD_3CN at 58°. Lines below the spectrum correlate N, H^{α}, and H chemical shifts as determined by spin decoupling experiments.

TABLE I: Spectral Assignments of the Proton Chemical Shifts and Coupling Constants for Antamanide-NaSCN (1:1.75) in CD_3CN at 58°.

	N	H^{α}	H^{β}	H^{γ}	$J_{H^{\alpha}H^{\beta}}$	$J_{H^{\beta}H^{\beta}}$	$J_{H^{N}H^{\alpha}}$
Ala	8.14	4.23	1.32				2.0
Phe	7.73	4.39	*a*				3.2
Phe	7.17	5.09	2.91, 2.60		8.5	14.5	
Val	6.91	4.51	1.83	0.98, 0.75			9.5
Phe	6.43	4.39	*a*		7.5, 11	10, 14.5	7.5
Phe	6.38	4.39	*a*				6.5
Pro		4.53	2.25		7.5, <2		
Pro		4.32	2.14				
Pro		4.16	2.36, 1.77		7.5, 7.5		
Pro		3.80	2.14				

[a] The three Phe C^{α} protons at 4.39 are coupled to C^{β} protons at 3.02, 2.91, and 2.84 ppm.

protons occur in pairs (similarity in chemical shifts and coupling constants) and could arise from the pseudosymmetry of the polypeptide, *i.e.*, those residues separated by four intervening residues may have similar backbone conformations (Val_1 and Phe_6; Ala_4 and Phe_9; Phe_5 and Phe_{10}). Thus, the Phe peptide NH resonance at 7.73 ppm ($J_{H^{N}H^{\alpha}}$ = 3.2 Hz) is assigned to Phe_9 on comparison with the Ala_4 peptide NH resonance at 8.14 ppm ($J_{H^{N}H^{\alpha}}$ = 2.0 Hz). The Phe peptide NH resonance at 7.17 ppm ($J_{H^{N}H^{\alpha}} \sim 10$ Hz) is assigned to Phe_6 on comparison with the Val_1 peptide NH resonance at 6.91 ppm ($J_{H^{N}H^{\alpha}}$ = 9.5 Hz). The remaining two Phe peptide resonances at 6.43 ($J_{H^{N}H^{\alpha}}$ = 7.5 Hz) and 6.38 ppm ($J_{H^{N}H^{\alpha}}$ = 6.5 Hz) are assigned to the symmetry-related phenylalanines at positions 5 and 10. The assignments are similar to those reported (Ivanov *et al.*, 1971).

TABLE II: Temperature Coefficients of the Peptide N Protons of Antamanide-NaSCN in CD_3CN, CD_3CO_2H, and Dimethylformamide (Ppm/°C × 10^3).

Solvent	Ala_4,Phe_9	Phe_6,Val_1	$Phe_{5/10}$
CD_3CN	4.1,4.0	0.8	1.4/3.8
CD_3CO_2H	5.1,5.4	1.7	0.8/4.0
$DCON(CD)_2$	4.1,4.1	2.4	6/11.3

The temperature dependences of the peptide NH resonances of the antamanide-Na complex in CD_3CN and CD_3CO_2H are shown in Figure 2 and their slopes in Table II. The peptide NH resonances of Val_1 and Phe_6, where observable, have small slopes ($\lesssim 2 \times 10^{-3}$ ppm/°C) suggesting their participation in short coplanar hydrogen bonds. The peptide NH resonances of Ala_4 and Phe_9 exhibit temperature coefficients of 4–5 × 10^{-3} ppm/°C and approach values ($\geq 6 \times 10^{-3}$ ppm/°C) typical of solvent-exposed protons. The temperature coefficients of Phe_5 and Phe_{10} are solvent dependent. In poor hydrogen-bond acceptor solvents (CD_3CN, CD_3CO_2H) the slopes are $\sim 1.2 \times 10^{-3}$ and 4 × 10^{-3} ppm/°C while in strong hydrogen-bond acceptor solvents (dimethylformamide) they exhibit larger values of 6 × 10^{-3} and 11.3 × 10^{-3} ppm/°C.

An exchange study was undertaken to investigate the accesibility to solvent of the peptide NH resonances of antamanide-Na in CD_3CN at 35°. The time course of the exchangeable resonances was followed on addition of 10% CD_3OD (Figure 3). The peptide NH resonances of Ala_4 and Phe_9 have half-lives for exchange of 1 hr while the peptide NH resonances of Val_1 and Phe_6 (by observation of its H^{α} resonance) remain unaffected after 4 days (Figure 3). Thus, the peptide NH reso-

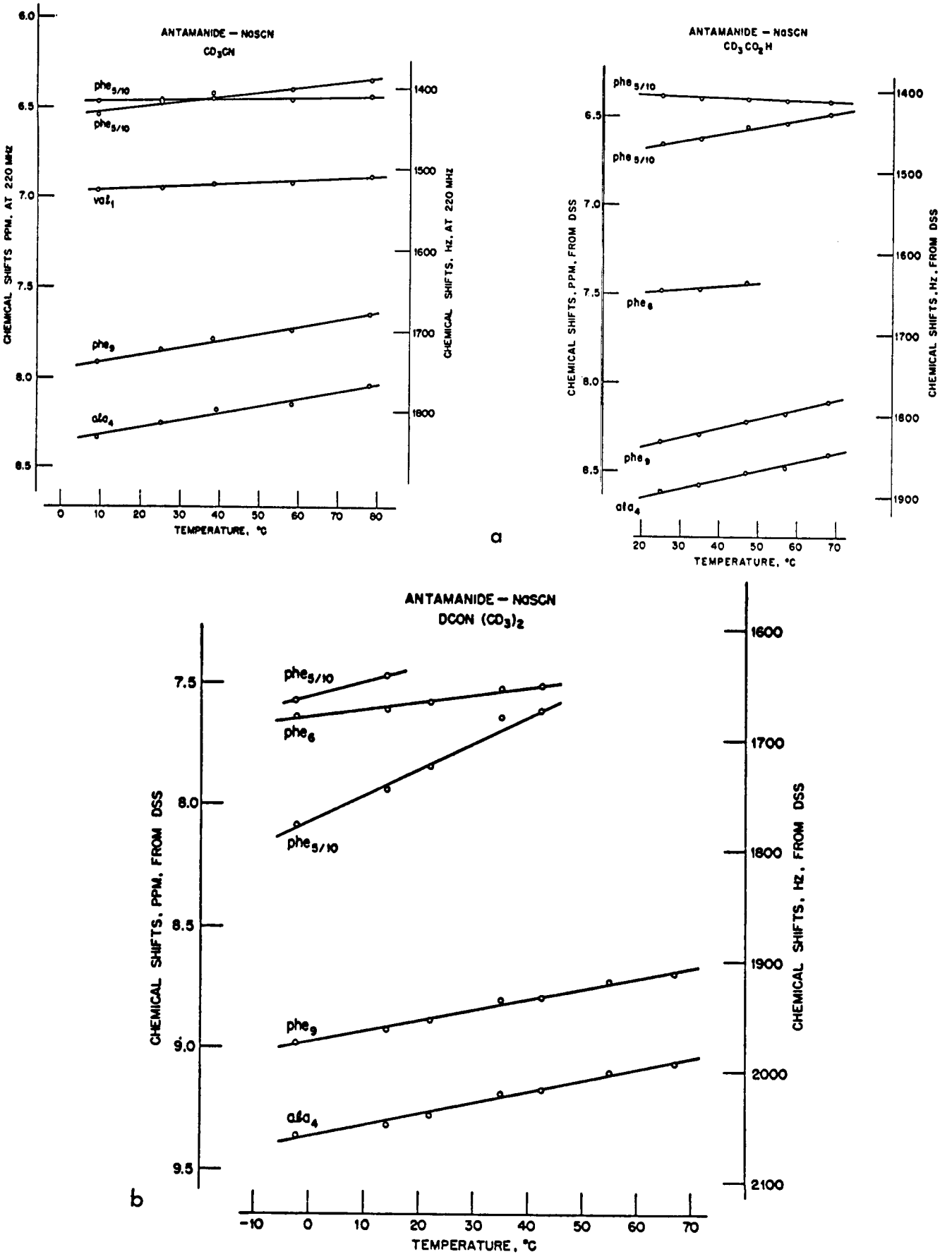

FIGURE 2: (a) Temperature coefficients of the peptide N protons of antamanide–Na in the weak hydrogen-bond acceptor solvents CD_3CN and CD_3CO_2H. (b) Temperature coefficients of the peptide N protons of antamanide–Na in the strong hydrogen-bond acceptor solvent dimethylformamide.

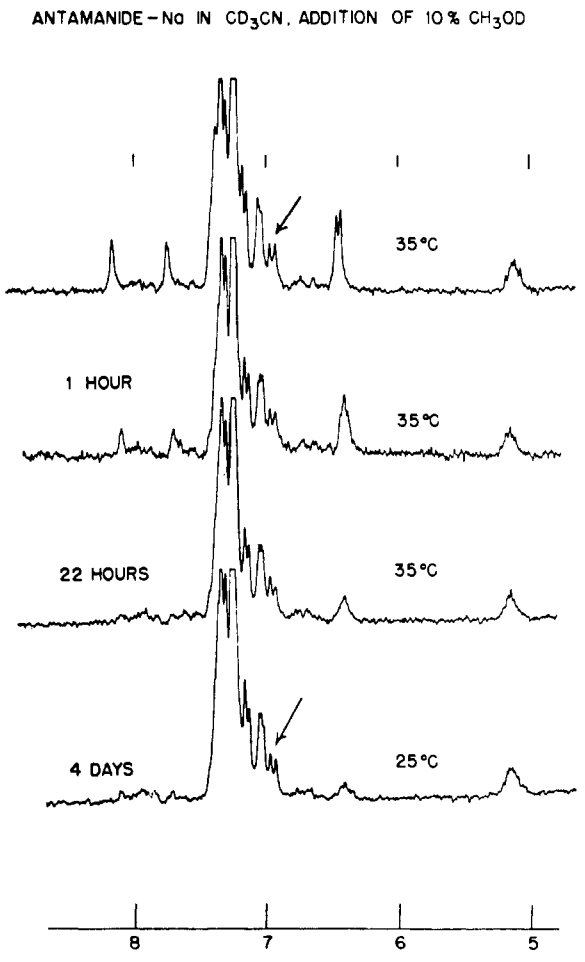

FIGURE 3: Time course for exchange of peptide N protons on addition of 10% CH_3OD to antamanide–Na in CD_3CN at 35°. The arrow indicates the peptide N proton of Val_1.

nances of Ala_4 and Phe_9 are exposed to solvent while those of Val_1 and Phe_6 participate in short coplanar intramolecular hydrogen bonds as suggested by the temperature coefficient data. The peptide NH resonances of Phe_5 and Phe_{10} have similar chemical shifts and possess intermediate exchange rates (Figure 3). It is proposed on the basis of the temperature coefficient and exchange data that the peptide NH resonances of Phe_5 and Phe_{10} are either solvent shielded or participate in weak intramolecular hydrogen bonds with the effect being more pronounced for one of these Phe residues.

The spectra of antamanide and antamanide–Na in CD_3CN are compared in Figure 4. Since both spectra have been extensively decoupled, a comparison in some detail can be made.

In the upfield region, the CH_3 resonance of Ala_4 (1.04 ppm) moves 0.3 ppm downfield and one of the Val_1 CH_3 resonances (0.96 ppm) moves 0.3 ppm upfield on complexation. In the 3.5–5-ppm region, the Phe_6 H^α resonance (4.47 ppm) is shifted downfield 0.6 ppm while the remaining three Phe H^α resonances are shifted (~0.2–0.6 ppm) on complexation to a common chemical shift of 4.39 ppm. On complexation, the peptide N protons of Ala_4 (7.83 ppm) and Phe_9 (7.47 ppm) move downfield ~0.3 ppm while those of Val_1 (7.02 ppm) and Phe_6 (~7.4 ppm) move upfield by 0.1–0.2 ppm. A large upfield shift (1 ppm) is noted for the peptide N protons of $Phe_{5/10}$ (~7.4 ppm) on formation of the complex (Figure 4).

In addition to the changes noted above, there are changes in the entire spectral range. In striking contrast, the H^α resonance of Val_1 (4.51 ppm) and Ala_4 (4.23 ppm) and one of Val_1 CH_3 groups (0.96 ppm) have the same chemical shifts in the two forms (Figure 4).

II. Na Exchange between Antamanide Molecules. Figure 5 outlines the effect on the nmr spectrum of antamanide in CD_3CN at 34° on gradual addition of NaSCN up to equimolar ratios of peptide to metal ion. Note that the spectra of antamanide and antamanide–Na (1:1) in CD_3CN exhibit narrow resonances while considerable broadening is observed throughout the spectral range at ratios of Na:antamanide of <1. Only the protons of H^α Val_1, H^α Ala_4, and Val_1 methyl do not broaden and this is ascribed to these protons having the same chemical shifts in the two forms. The broadening results from Na exchange between antamanide molecules

$$\text{antamanide–Na} + \textit{antamanide} \rightleftarrows \text{antamanide} + \textit{antamanide–Na}$$

(The binding constant for complexation in CD_3CN is 30,000 and all the Na is expected to be in the complexed form (Wieland *et al.*, 1972.) Let τ represent the average lifetime and δ_i represent the chemical-shift difference of proton i between the antamanide and antamanide–Na structures. The condition, $\tau^{-1} \ll \pi\delta_i$ (very slow exchange), is not valid in this case since separate narrow resonances were not observed at 34° for the two forms. Depending on the value of δ_i for a particular proton i the exchange is on the slow or fast side of the intermediate exchange condition ($\tau^{-1} \approx \pi\delta_i$). The large values of δ_i (= 1 ppm), observed for the peptide N protons of $Phe_{5/10}$, result in broad resonances at the chemical shifts of the two forms (note in Figure 5 at antamanide:Na = 1:0.5 a broad resonance at 6.4 ppm, corresponding to the positions of the N protons of $Phe_{5/10}$ in the complex). On the other hand, for a smaller value of δ_i (= 0.3 ppm), observed for the methyl resonance of Ala_4, an average exchange-broadened resonance shifts with Na ion concentration from 1 to 1.3 ppm.

The binding of Na ion to the cyclic ether, dibenzo-18-crown-6 (DBC), has been investigated as a function of metal ion concentration. The exchange resulted in maximum broad-

$$\textit{DBC}\text{–Na} + \text{DBC} \rightleftarrows \textit{DBC} + \text{DBC–Na}$$

ening at Na:DBC = 0.5. The temperature-dependent line widths yielded an activation energy of 12.5 kcal/mol (Wong *et al.*, 1970). This system has also been investigated in the presence of excess Na. The exchange (equilibrium constant ~600 M^{-1}) yielded activation energies of complexation and

$$\text{Na} + \text{DBC} \rightleftarrows \text{Na–DBC}$$

decomplexation of 6.5 and 12.5 kcal/mol, respectively (Shchori *et al.*, 1971).

III. The X-Pro Peptide Bond. For imino acids, like proline, the X-Pro peptide bond may be cis or trans. This section evaluates the experimental evidence on X-Pro bond geometry for the antamanide–Na complex.

The Gly-Pro peptide bonds are cis for *cyclo*(Gly-Pro)$_3$ in methylene chloride while the Gly-Pro peptide bonds are trans for the Na complex of this cyclic peptide. Gradual addition of NaSCN to *cyclo*(Gly-Pro)$_3$ (Na/peptide < 1) resulted in sharp resonances for the cyclic peptide and its Na complex, consistent with a 20-kcal barrier to cis–trans peptide bond isomerization (Deber *et al.*, 1972).

The line-width effects (mentioned in the previous section) on gradual addition of NaSCN to antamanide arise from Na exchange between antamanide and its complex without cis–

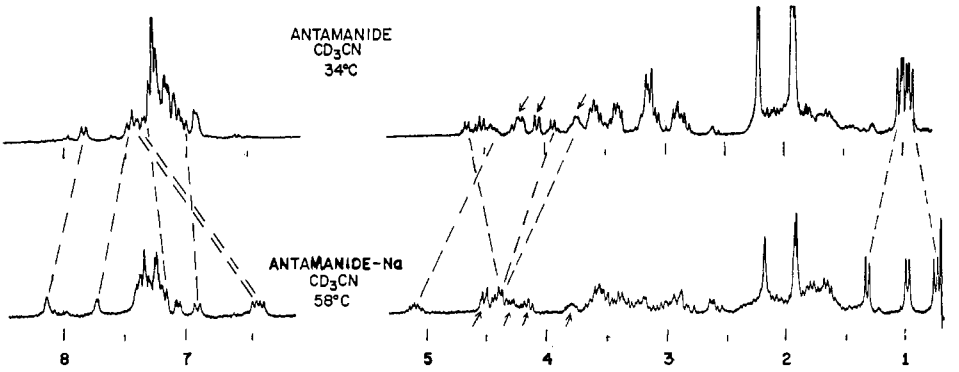

FIGURE 4: Comparison of the proton nmr spectra of antamanide and antamanide–Na in CD_3CN. The arrows indicate the position of Pro H^{α} protons. The dashed lines between 3.5 and 5 ppm indicate the chemical-shift changes on complexation for four Phe H^{α} protons.

trans peptide bond isomerization. A 20-kcal/mol barrier per peptide bond isomerized would be manifested as separate narrow resonances for antamanide and its complex (Na/peptide < 1), a feature not observed experimentally in CD_3CN at 34° (Figure 5).

Conformations for antamanide in CD_3CN in the previous manuscript were generated with cis peptide bonds at Val_1-Pro_2 and Phe_6-Pro_7 in one case and at Pro_2-Pro_3 and Pro_7-Pro_8 in another case. The Na exchange studies suggest that two cis X-Pro peptide bonds at these same positions must be considered for the Na complex of antamanide.

In the previous manuscript the Pro H^{α} splitting patterns and chemical shifts were used to indicate whether the X-Pro peptide bond exhibited the cis or trans geometry (Patel, 1973). From model system studies, a cis X-Pro peptide bond exhibited $J_{H^{\alpha}H^{\beta}} = 7.0$ and 1.4 Hz, *i.e.*, a doublet for Pro H^{α} proton (Torchia *et al.*, 1972a,b; Deber *et al.*, 1971; Deber *et al.*, 1972; Kopple, 1971), while a trans X-Pro peptide bond exhibited $J_{H^{\alpha}H^{\beta}} = 8.5$ and 5.5 Hz, *i.e.*, a multiplet for Pro H^{α} proton (Torchia, 1971; Deber *et al.*, 1972; Torchia, 1972; Torchia *et al.*, 1972a,b), with the cis peptide Pro H^{α} proton appearing downfield from its trans peptide analog. The four Pro H^{α} protons in antamanide–Na in CD_3CN at a series of temperatures are shown in Figure 6. The Pro H^{α} resonance at 4.16 ppm is a triplet while the one at 3.80 ppm is a multiplet, indicating trans X-Pro peptide bonds. The proline H^{α} resonances at 4.53 and 4.32 ppm are superimposed with other resonances. On lowering the temperature, the Pro H^{α} proton at 4.53 ppm can be separated from the Val H^{α} proton triplet. This downfield Pro H^{α} resonance exhibited $J_{H^{\alpha}H^{\beta}} \sim 8$ and 2.5 Hz making an assignment to cis or trans X-Pro peptide bond difficult. Thus, of the four prolines in the complex, two have trans X-Pro peptide bonds while the geometry at the X-Pro peptide bond for the other two prolines cannot be defined by the above analysis.

The heteronoise proton-decoupled ^{13}C spectrum of antamanide–NaSCN in CD_3CN at 50° is outlined in Figure 7. Chemical shifts are referenced relative to CS_2 and assignments are made by comparison with amino acid spectra. The assignments are summarized in Table III.

In the previous manuscript the sensitivities of C^{β} and C^{γ} Pro carbon shifts to the cis or trans nature of the X-Pro peptide bond were outlined (Patel, 1973). For cis and trans X-Pro peptide bonds, the proline C^{γ} resonances have chemical shifts at 170.4 ± 0.3 and 168.5 ± 0.3 ppm, respectively, in the model systems. This permits assignment of antamanide–Na proline C^{γ} resonances at 170.1 and 169.7 ppm to cis X-Pro peptide bonds while the proline C^{γ} resonances at 168.0 and 167.2 ppm are assigned to trans X-Pro peptide bonds (Table III). For cis and trans X-Pro peptide bonds, the proline C^{β} reso-

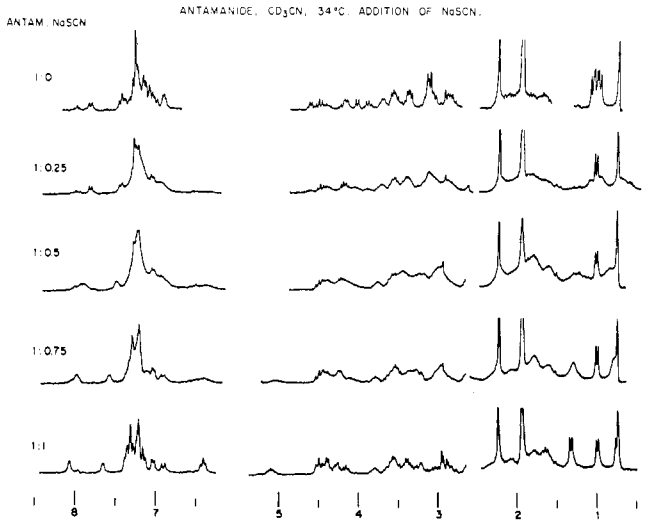

FIGURE 5: The proton nmr spectra of antamanide in CD_3CN at 34° on gradual addition of NaSCN.

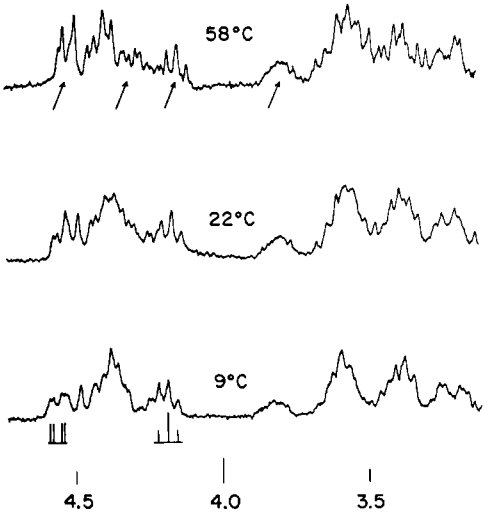

FIGURE 6: The H^{α} proton region of the proton nmr spectrum of antamanide–NaSCN in CD_3CN at three temperatures. The arrows indicate the position of Pro H^{α} proton resonances.

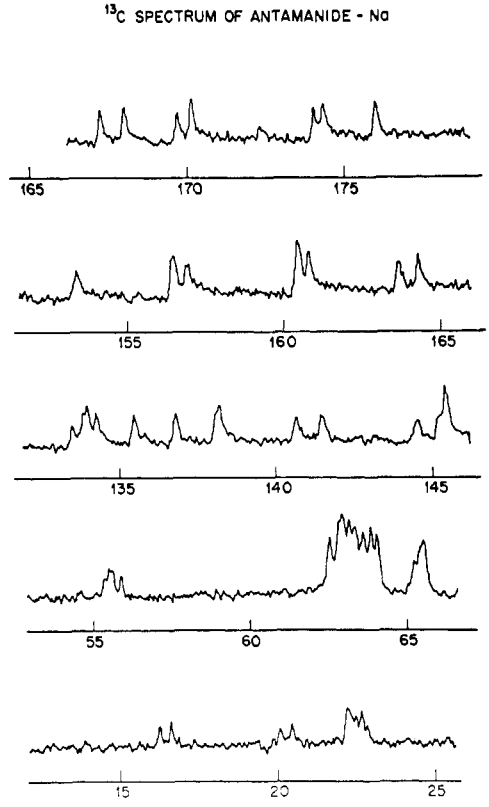

FIGURE 7: The heteronoise proton-decoupled ^{13}C spectrum of antamanide–NaSCN in CD_3CN at 50°.

nances have chemical shifts at 161.5 ± 0.4 and 163.8 ± 1.1 ppm, respectively, in model systems. This permits assignment of antamanide–Na proline C^{β} resonances in the region 160.7 ± 0.2 ppm to cis X-Pro peptide bonds while the proline C^{β} resonances at 164.3 and 163.7 ppm are assigned to trans X-Pro peptide bonds (Table III). *The ^{13}C nmr data strongly suggest that two X-Pro peptide bonds are cis and two are trans for antamanide–Na in CD_3CN.*

The $\pi \rightarrow \pi^*$ 190–205-nm CD band for perhydroantamanide in methanol exhibits a molar rotation of −70,000 deg cm²/dmol. On complexation with NaSCN this band exhibits $[\theta]_M$ = −150,000 deg cm²/dmol (Faulstich *et al.*, 1972). The increase in negative rotation in the $\pi \rightarrow \pi^*$ band on complexation may be due either to a large conformational change or to cis → trans isomerization at an X-Pro peptide bond or due to coordination of carbonyl oxygens to sodium.

In summary, the ^{13}C spectra in the C^{β} and C^{γ} region of the complex as well as the results of gradual addition of NaSCN to antamanide suggest the presence of two cis and two trans X-Pro bonds for antamanide–sodium in solution. On the other hand, studies of the multiplicity of the H^{α} proline proton resonances in the complex and the rotational change on complexation for the $\pi \rightarrow \pi^*$ 190–205-nm CD band of perhydroantamanide are inconclusive as to the nature of the X-Pro peptide bonds in the complex.

IV. Generation of Complex Conformations. In this section several conformations are generated for the structure of the antamanide–Na complex in solution. In generating conformations of antamanide–Na, several considerations have to be evaluated. The overall conformational energy of the complex comprises (i) the favorable interaction between the positively charged ion and the carbonyl oxygens, (ii) the unfavorable interactions among the cluster of carbonyl groups forming the cavity, and (iii) the conformational energy of the polypeptide. Thus, it may be suggested that a high conformational energy of the polypeptide backbone may be compensated for by the Na–carbonyl interaction giving a low conformational energy for the complex. However, not enough information is currently available to evaluate effects i and ii and thus only those conformations of the polypeptide possessing low conformational energy for the backbone are considered in this article.

TABLE III: Spectral Assignments of the ^{13}C Chemical Shifts (Ppm Relative to CS_2) for Antamanide–Sodium in CD_3CN at 50°.

CH_3, Ala,Val	176.0, 174.3, 174.1
C^{γ}, Pro	170.1, 169.7, 168.0, 167.2
C^{β}, Pro	164.3, 163.7
C^{β}, Pro,Val	160.9, 160.5, 160.5
C^{β}, Phe	157.0, 156.5, 156.4, 153.3
C^{δ}, Pro	145.5, 145.5, 145.3, 144.7
C^{α}, Ala,Phe	141.4, 140.7
C^{α}, Phe	138.2, 138.1
C^{α}, Phe,Val	136.8, 135.4
C^{α}, Pro	134.2, 133.9, 133.8, 133.5

The following procedure was utilized in defining the solution conformation(s) of the antamanide–Na complex. Using the Corey–Pauling–Koltun (CPK) models a conformation of the complex consistent with all the conditions required by the nmr data and conformational energy maps discussed above, and which possessed a cluster of four–six carbonyls capable of binding Na ion (ionic radius = 0.97 Å), was generated. Since K ion (ionic radius = 1.33 Å) has a smaller binding constant by an order of magnitude the dimensions of the cavity and/or accessibility to and from the cavity are specific for Na ion.

For a tetrapeptide sequence containing L residues and trans peptide bonds a type I bend can be generated, stabilized by a 1 ← 4 intramolecular hydrogen bond. Venkatachalam (1968)

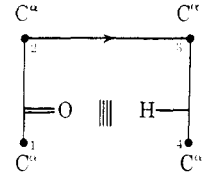

has shown from conformational calculations that $\varphi_2 \sim 120$, $\psi_2 \sim 140$, and $\varphi_3 \sim 60$, $\psi_3 \sim 240$ constitutes lowest energy conformation for a type I bend involving L-amino acids other than glycine at positions 2 and 3 (see Ramachandran *et al.*, 1970, for further details). These rotation values predict a small $J_{H^NH^{\alpha}}$ (<3 Hz) for residue 2 and a large $J_{H^NH^{\alpha}}$ (7–10 Hz) for residue 3.

From decoupling, temperature coefficient, and exchange studies on the antamanide–Na complex in solution it was

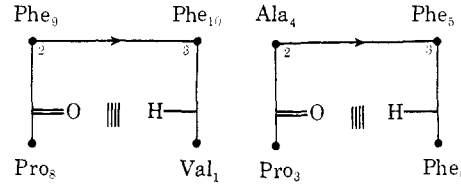

TABLE IV: Rotation Angles φ, ψ, and ω for Conformations *trans*-Complex, 2,7-*cis*-Complex, and 1,6-*cis*-Complex, Candidates for the Antamanide–Sodium Conformation in Solution.[a]

	Val_1,-Phe_6	Pro_2,-Pro_7	Pro_3,-Pro_8	Ala_4,-Phe_9	Phe_5,-Phe_{10}
trans-Complex φ	60	120	120	120	90
ψ	330	330	120	120	240
ω	0	0	0	0	0
2,7-*cis*-Complex φ	60	120	120	120	90
ψ	330	330	330	120	240
ω	0	180	0	0	0
1,6-*cis*-Complex φ	30	120	120	120	90
ψ	330	360	120	120	120
ω	180	0	0	0	0

[a] Rotation angle convention according to Edsall *et al.* (1966).

shown that the peptide N protons of Val_1 and Phe_6 form short coplanar intramolecular hydrogen bonds and that of Ala_4 and Phe_9 exhibited small $J_{H^NH^\alpha}$ (<3 Hz). Thus, for the complex, the type I bends designated below are consistent with the nmr data. The φ, ψ, and ω angles for the residues Ala_4,Phe_9 (position 2 in type I bend) and Phe_5,Phe_{10} (position 3 in type I bend) are tabulated below.

	Ala_4,Phe_9	Phe_5,Phe_{10}
φ, deg	~120	~60
ψ, deg	~140	~240
ω, deg	0	0

The antamanide sequence contains prolines at positions 2, 3, 7, and 8. The pyrrolidine ring fixes the φ values of Pro_2,Pro_7 at ~102° and Pro_3,Pro_8 at ~122° according to the crystallographic analysis of poly-L-proline-II (Cowan and McGavin, 1955; Sasisekharan, 1959) and L-leucyl-L-prolylglycine (Leung and Marsh, 1958), respectively. ψ values of Pro_2 = Pro_7 = 310° and Pro_3 = Pro_8 = 125° or 325° are chosen and correspond to calculated energy minima (Schimmel and Flory, 1967, 1968) for an L-prolyl residue succeeded by another L-prolyl residue, and an L-prolyl residue succeeded by any residue other than prolyl, respectively. The allowed φ and ψ values for the prolines are summarized below.

	Pro_2,Pro_7	Pro_3,Pro_8
φ, deg	~102	~122
ψ, deg	~310	~125 or ~325

Since Val_1 and Phe_6 have large values of $J_{H^NH^\alpha}$ (10 Hz) their φ values are restricted to 60 and 240° from the Karplus correlation between $J_{H^NH^\alpha}$ and dihedral angle φ (Barfield and Karplus, 1969). Corresponding low-energy values of ψ for Val_1 and Phe_6 are in the range 270–330° from conformational energy maps for a residue X in an X-Pro sequence.

As stated above, the variables not fixed by the nmr data are the Val_1 and Phe_6 φ values which can have the rotation angles 60 or 240°, the Pro_3 and Pro_8 ψ values which can have rotation angles in the range 270–330 or 120–150, and the geometry at the X-Pro peptide bonds which can have either cis or trans configuration. All the conformations for the complex described below were generated from model building studies.

A conformation with all-trans peptide bonds was generated for the complex with ψ values for Pro_3 = Pro_8 ~ 125° and φ values for Val_1 = Phe_6 ~ 60° (see Table IV). This conformation, designated the *trans*-complex, has four carbonyl oxygens (Pro_2, Pro_7, Val_1, Phe_6) arranged in a tetrahedral geometry and the cavity is specific for Na ion (plate 1).

A conformation with cis X-Pro peptide bonds at Pro_2-Pro_3 and Pro_7-Pro_8 was generated for the complex with ψ values for Pro_3 = Pro_8 ~ 330° and φ values for Val_1 = Phe_6 ~ 60° (see Table IV). This conformation is designated the 2,7-*cis*-complex. The carbonyl oxygens of Val_1, Phe_6, Ala_4, and Phe_9 possess the geometry for complexing the metal ion (plate 2). In addition, the carbonyls of Pro_2, Pro_7, Pro_3, and Pro_8 may form part of the cavity.

A conformation with one cis X-Pro peptide bond at Pro_2-Pro_3 was generated for the complex with ψ values for Pro_3 ~ 125° and Pro_8 ~ 360° and φ values for Val_1 = Phe_6 ~ 60° (conformation 2-*cis*-complex). Similarly, a conformation with one cis X-Pro peptide bond at Pro_7-Pro_8 was generated with ψ values for Pro_3 ~ 360° and Pro_8 ~ 125° and φ values for Val_1 = Phe_6 ~ 60° (conformation 7-*cis*-complex). Both these conformations lack a pseudotwofold symmetry axis but do exhibit a cavity for binding metal ion.

Conformation 1,6-*cis*-I, suggested in the previous manuscript (Patel, 1973) as a structure for antamanide in poor hydrogen-bond acceptor solvents, exhibited a cluster of four carbonyls (Ala_4, Phe_5, Phe_9, and Phe_{10}). Starting with this conformation, an attempt was made to generate the complex, keeping the geometry at the peptide bonds unchanged.

Since the peptide NH resonances of Val_1 and Phe_6 participate in short coplanar intramolecular hydrogen bonds (temperature coefficient data) for both 1,6-*cis*-I and the complex, the geometry at these residues was kept the same on complexation (*i.e.*, peptide NH of Val_1 hydrogen bonded to carbonyl of Phe_6 and peptide NH of Phe_6 hydrogen bonded to carbonyl of Val_1).

For a tetrapeptide sequence of L-amino acids and trans peptide bonds, a bend stabilized by a short coplanar 1 ← 4 intramolecular hydrogen bond can be generated with φ,ψ = 120,150° for residues at positions 2 and 3 (Venkatachalam,

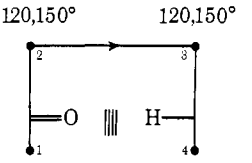

1968). The complex was generated with two such modified bends with φ and ψ rotation angles of 120 and 120° at positions 2 and 3. In this modified bend, the NH and OC groups

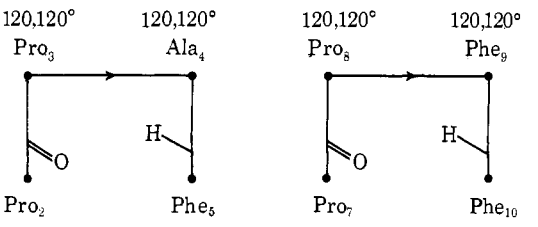

are not coplanar. The rotation angles for the conformation of the complex, designated the 1,6-*cis*-complex, are summarized in Table IV. The φ values are consistent with experimental $J_{H^NH^\alpha}$ coupling constants and ψ values in the range 280–360°

are consistent for an X residue (Val_1,Phe_6,Pro_2,Pro_3) in an X-Pro sequence. The cavity is lined with eight carbonyls, four of which exhibit the geometry for complexing the metal ion. CPK models of this conformation are shown in plate 3.

V. Evaluation of Chemical-Shift Changes on Complexation. The conformations proposed for the antamanide–sodium complex must explain qualitatively most of the striking chemical-shift changes observed on addition of Na ion to antamanide in solution.

Since the *trans*-complex, 2,7-*cis*-complex, 2-*cis*-complex, and 7-*cis*-complex conformations were constructed starting with identical bends, they will be considered first. The two type I bends stabilized by 1 ← 4 intramolecular hydrogen bonds involve all the six peptide NH protons and the Ala_4 and Val_1 methyl groups. One possible orientation of phenyl rings at positions 5, 9, and 10 in 2,7-*cis*-complex is shown in plate 4. In this orientation, the methyl group of Ala_4 is close to and in the plane of the aromatic ring of Phe_5 and the expected downfield shift on complexation is observed experimentally (plate 4, model on right). One of the Val_1 methyl groups is in the shielding region of the aromatic ring of Phe_{10} and an upfield shift of this group is predicted as observed experimentally (plate 4, model on left).

The H^α protons of Ala_4, Phe_5, Phe_9, and Phe_{10} have the same spatial relationship relative to the metal ion cavity but not with respect to the carbonyl groups in their vicinity (plate 2, model on left). These residues exhibit almost identical H^α chemical shifts in the complex (Table I, Figure 4). The above arguments are valid for *trans*-complex, 2,7-*cis*-complex, 2-*cis*-complex, and 7-*cis*-complex since the φ,ψ rotation angles for the non-proline residues are the same for these conformations (see Table IV). These conformations differ as to the number of cis X-Pro peptide bonds and the φ,ψ values at Pro_3,Pro_8. The spatial arrangement of groups around Pro_2,Pro_7 is similar as is the environment around Pro_3,Pro_8 in the CPK models of *trans*-complex and 2,7-*cis*-complex, and should be reflected in the chemical shift of the proline H^α protons. Experimentally, the four proline H^α protons do not appear in pairs but resonate at 4.53, 4.32, 4.16, and 3.80 ppm. This may arise from ring current effects of the four phenyl rings. In the conformations with one cis peptide bond, 2-*cis*-complex and 7-*cis*-complex, all four proline H^α protons are in different structural environments.

For 1,6-*cis*-complex conformation, one of the Val_1 methyl groups can be shielded by the aromatic ring of Phe_{10} while the Ala_4 methyl group can be deshielded by the aromatic ring of Phe_5. The arrangement of carbonyl groups in the vicinity of the H^α carbons of Ala_4, Phe_9, Phe_5, and Phe_{10} is close to the same as is their distance from the center of the cavity consistent with identical chemical shifts of the H^α resonances of these residues.

VI. Comparison of 2,7-cis-Complex and 1,6-cis-Complex Conformations. In the previous article, the conformations of antamanide in nonaqueous solution were represented by one of two possibilities (Patel, 1973): 2,7-*cis*-I ⇄ 2,7-*cis*-II; 1,6-*cis*-I ⇄ 1,6-*cis*-II.

Since the gradual addition of NaSCN did not result in cis–trans peptide bond isomerization (no doubling of spectra) the best candidates for the structure of the complex are 2,7-*cis*-complex and 1,6-*cis*-complex. Features of their conformations are compared below.

The antamanide H^α proton chemical shifts of Val_1 and Ala_4 remain unchanged on complexation with NaSCN in CD_3CN. For the conversion 2,7-*cis*-I → 2,7-*cis*-complex, the orientation of carbonyl groups around Val_1 H^α remains unchanged while the orientation of carbonyl groups around Ala_4 H^α changes on complexation. For the conversion 1,6-*cis*-I → 1,6-*cis*-complex, the orientation of carbonyl groups around both Val_1 and Ala_4 H^α remains unchanged on complexation, in agreement with the experimental observation.

From temperature coefficient (Figure 2, Table II) and exchange studies (Figure 3), the peptide N protons of Phe_5 and Phe_{10} exhibit properties that are intermediate to those of the intramolecularly hydrogen-bonded peptide N protons of Val_1 and Phe_6 and the solvent-exposed peptide N protons of Ala_4 and Phe_9. For conformation 2,7-*cis*-complex, this intermediate behavior for the peptide N protons of Phe_5 and Phe_{10} may be attributed to shielding from solvent by the aromatic rings. These exchangeable protons are shown in plate 4 and their solvent-shielded nature remains questionable. For conformation 1,6-*cis*-complex, the peptide N protons of Phe_5 and Phe_{10} form weak nonlinear intramolecular hydrogen bonds with the carbonyls of Pro_2 and Pro_7 and in addition may be shielded from solvent by Pro and Phe side chains. A combination of these effects is consistent with the intermediate exchange rates and temperature coefficients observed experimentally.

The Phe_5 and Phe_{10} peptide N protons for antamanide in CD_3CN shift 1 ppm upfield on complexation with NaSCN (Figure 4). No satisfactory explanation other than shielding by the phenyl rings in the complex can be put forward for the 2,7-*cis*-complex. On the other hand, it has been documented (Stern *et al.*, 1968; Urry and Ohnishi, 1972; Torchia *et al.*, 1972a,b) that the peptide protons participating in type 1 ← 4 intramolecular hydrogen bonds come upfield from other peptide N protons as a result of the shielding by the peptide bond between residues 2 and 3. For 1,6-*cis*-complex, the peptide NH resonances of Phe_5 and Phe_{10} form weak nonlinear type 1 ← 4 intramolecular hydrogen bonds and these protons are shielded by the peptide bonds of Pro_3-Ala_4 and Pro_8-Phe_9, respectively. The conformation 1,6-*cis*-complex readily ac-

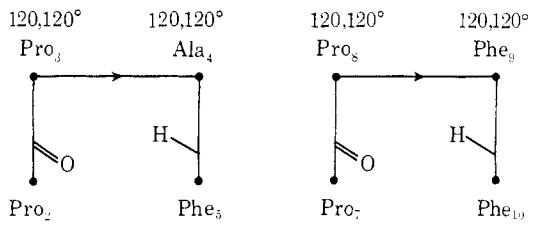

counts for the upfield shifts observed experimentally.

The peptide NH resonances for antamanide–Na exhibit solvent-dependent chemical shifts (Figure 8). The shifts are similar in weak hydrogen bond acceptor nonaqueous solvents like CD_3CN and CD_3CO_2H, but are drastically different in dimethylformamide, a strong hydrogen-bond acceptor nonaqueous solvent. In dimethylformamide, the weak nonlinear intramolecular hydrogen bonds for peptide NH resonances of Phe_5 and Phe_{10} in 1,6-*cis*-complex are broken and hydrogen bonds to solvent are formed. These resonances are no longer shielded by the peptide groups and they move downfield.

As stated in the previous article (Patel, 1973), antamanide conformation 2,7-*cis*-I does not exhibit a cluster of carbonyls that can serve as a recognition site for the metal ion. Furthermore, Val_1 and Phe_6 form short coplanar intramolecular hydrogen bonds to the carbonyls of Ala_4 and Phe_9, respectively, in 2,7-*cis*-I and the carbonyls of Pro_8 and Pro_3, respectively, in 2,7-*cis*-complex. Thus, complexation would require the breakage and formation of new intramolecular hydrogen bonds. On the other hand, antamanide conformation 1,6-*cis*-I exhibits a cluster of four carbonyls (Ala_4, Phe_5, Phe_9, and

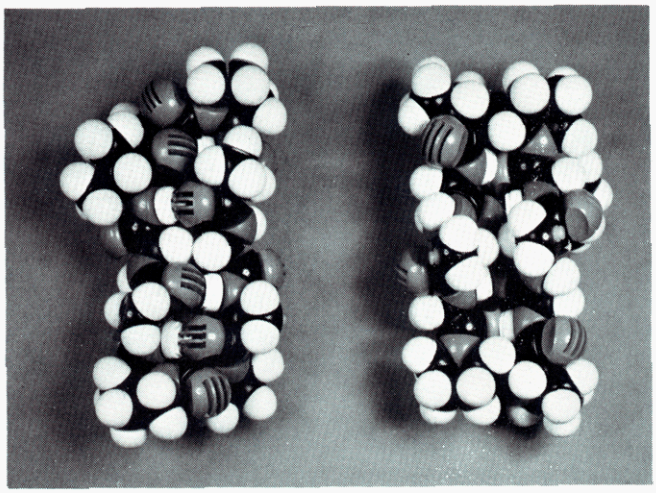

PLATE 1 (Amide Conformation in Nonaqueous Media): Corey–Pauling–Koltun models of conformation 2,7-cis-I. Phenyl rings omitted for sake of clarity.

PLATE 2 (Amide Conformation in Nonaqueous Media): Corey–Pauling–Koltun models of conformation 1,6-cis-I. Phenyl rings omitted for sale of clarity.

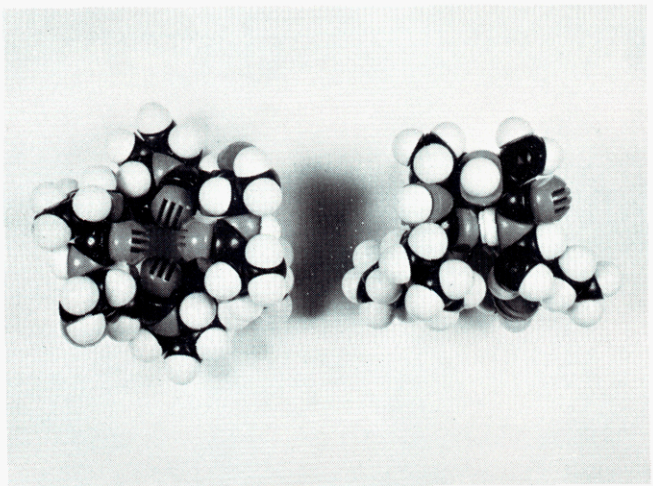

PLATE 2 (Conformation of Antamanide–Sodium in Solution): Two views of the Corey–Pauling–Koltun model of conformation 2,7-cis complex. The view on the left indicates the cavity while the view on the right presents type I bend stabilized by intramolecular 1←4 hydrogen bond. Phenyl rings omitted for clarity.

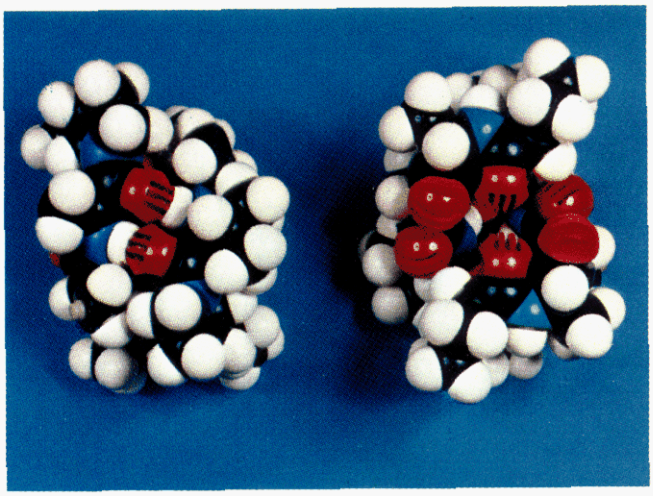

PLATE 3 (Conformation of Antamanide–Sodium in Solution): Two views of the Corey–Pauling–Koltun model of conformation 1,6-cis complex. The view on the right indicates the cavity while the view on the left shows two intramolecular hydrogen bonds. Phenyl rings omitted for clarity.

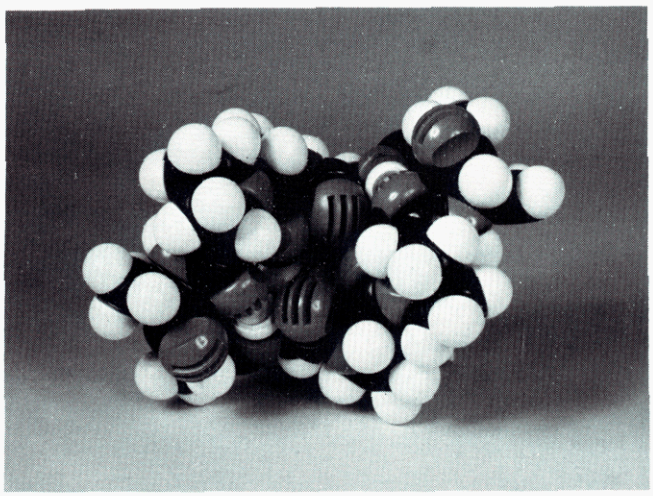

PLATE 1 (Conformation of Antamanide–Sodium in Solution): Corey–Pauling–Koltun model of conformation trans complex. This view outlines the cavity and two type I bends. Phenyl rings omitted for clarity.

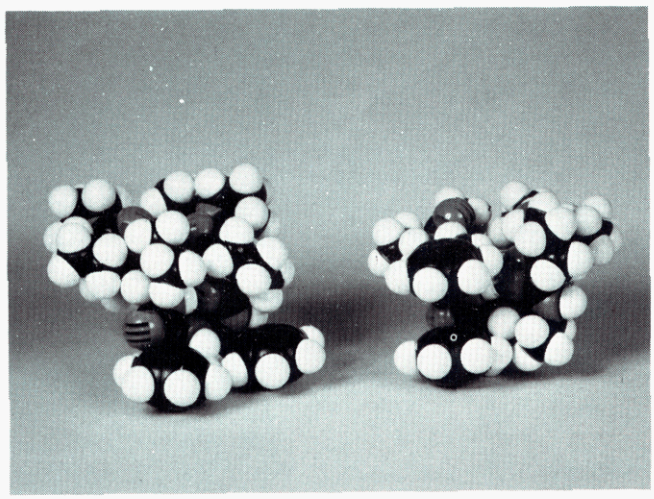

PLATE 4 (Conformation of Antamanide–Sodium in Solution): Two views of a Corey–Pauling–Koltun model of 2,7-cis complex. The model on the left shows one of the Val_1 methyl groups shielded by the aromatic ring of Phe_{10}. The model on the right shows the Ala_4 methyl group deshielded by the aromatic ring of Phe_3.

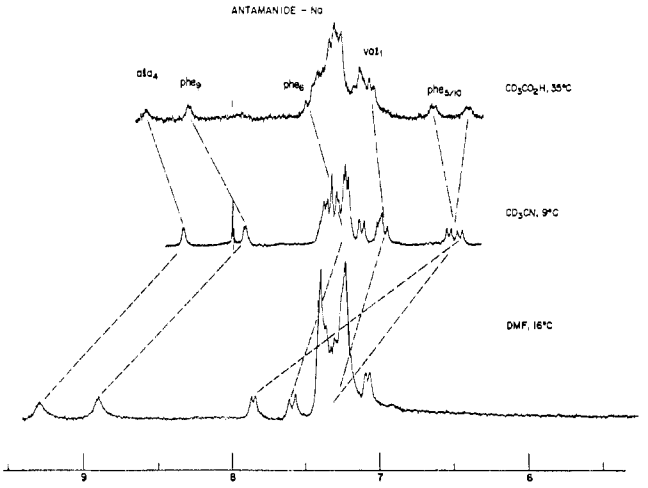

FIGURE 8: The solvent dependence of the chemical shifts of the peptide N protons of antamanide–NaSCN in solution.

Phe_{10}) that may serve as a recognition site for metal ion (see plate 3, model on right). Further, Val_1 and Phe_6 form short coplanar intramolecular hydrogen bonds to the carbonyls of Phe_6 and Val_1, respectively, in both 1,6-*cis*-I and 1,6-*cis*-complex suggesting that complexation can proceed with no change at these residues.

Conformations 2,7-*cis*-complex and 1,6-*cis*-complex exhibit cavities for complexation with metal ions. For 2,7-*cis*-complex, all the carbonyls except those of Phe_5 and Phe_{10} are close to the metal ion. The size of the cavity is selective for the Na ion (ionic radius, 0.95 Å). For 1,6-*cis*-complex, all ten carbonyls are close to the metal ion, though only the carbonyls of Pro_2, Pro_7, Pro_3, and Pro_8 are involved in the coordination. The cavity is quite large but the selectivity of Na ion over the larger alkali cations is attributed to limited access for entry and departure of the metal ion by the ten carbonyls lining the cavity.

The carbonyl groups coordinated to a positively charged metal ion should exhibit downfield ^{13}C chemical shifts compared to the uncomplexed form. The ^{13}C nmr spectrum of the carbonyl region for antamanide–Na in CD_3CN at 50° is shown in Figure 7. It is clear that four carbonyls are shifted downfield in pairs. Since the positions of these carbonyl carbons are not known with certainty in the uncomplexed form, the magnitude of the shift remains undetermined.

The experimental evidence appears to be more consistent with 1,6-*cis*-complex for the conformation of antamanide–Na in solution.

VII. Conformation trans-Complex-M. An Evaluation. As stated in the introductory statement, a conformation designated *trans*-complex-M has been reported by Ivanov *et al.* (1971) for antamanide–Na in solution, with the rotation angles tabulated in Table V. This conformation is reviewed critically in this section.

A value of $\psi = 310°$ is predicted from energy calculations (Schimmel and Flory, 1967) for an L-prolyl residue succeeded by another L-prolyl residue and observed experimentally for polyproline I, polyproline II, and model fragments containing proline sequences (Cowan and McGavin, 1955; Sasisekharan, 1959). Thus, the assignment $\psi_{Pro_2} = \psi_{Pro_7} = 130°$ for *trans*-complex-M predicts a very high conformational energy. By contrast, Go and Scheraga (1970) have pointed out that the first Pro in a Pro-Pro sequence may exhibit $\psi = 120°$ if a flexible geometry is permitted for the Pro ring.

TABLE V

	Val_1,Phe_6	Pro_2,Pro_7	Pro_3,Pro_8	Ala_4,Phe_9	Phe_5,Phe_{10}
φ, deg	80	120	120	330	250
ψ, deg	20	130	270	150	110

The temperature coefficient and exchange studies are consistent with short coplanar intramolecular hydrogen bonds for the peptide N protons of Val_1 and Phe_6. For conformation *trans*-complex-M these residues participate in long nonlinear type 1 ← 3 intramolecular hydrogen bonds.

There are two bends stabilized by the 1 ← 4 intramolecular hydrogen bond for *trans*-complex-M and they are depicted below. Conformational calculations predict, for the case of

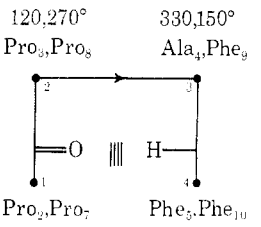

Pro at position 2 and an L-amino acid at position 3, that the bend stabilized by the type 1 → 4 intramolecular hydrogen bond can be made in two ways (Tonelli, 1973)

	Residue 2	Residue 3
Type I	130,140°	60,240°
Type II	120,280°	240,220°

It is apparent that $\varphi,\psi = 330,150°$ predicted for Ala_4-Phe_9 at position 3 does not meet the requirement of either type I or type II bends. Furthermore, $\varphi,\psi = 330,150°$ does not correspond to a low-energy residue conformation in the energy maps derived from approximate intramolecular potential energy calculations (Brant and Flory, 1965; DeSantis *et al.*, 1965; Ramakrishnan and Ramachandran, 1965). The peptide N protons of Phe_5 and Phe_{10} form short coplanar type 1 ← 4 intramolecular hydrogen bonds in the bends depicted above and would be expected to form the strongest hydrogen-bonded protons in the complex. Experimentally, the peptide N protons of Val_1 and Phe_6 form the strongest hydrogen bonds both from temperature and exchange studies. However, antamanide, N-alkylated at Val_1 and Phe_6, exhibits a greater binding constant for Na ion than antamanide itself (Ovchinnikov 1972).[1]

Finally, Phe_5 and Phe_{10} have been assigned φ,ψ values of 250,110°. Quantum mechanical calculations predict a low conformational energy for this region (Pullman and Maigret, 1972) as do the calculations of Crippen and Scheraga (1970) and experimental evidence supporting this orientation has been put forward for dipeptides (Bystrov *et al.*, 1969).

Summary of Conclusions

The proton nmr spectra parameters (chemical shifts and coupling constants) have been assigned for antamanide–Na in solution. Temperature coefficient and exchange studies sug-

[1] Ovchinnikov, Yu. A. (1972), private communication.

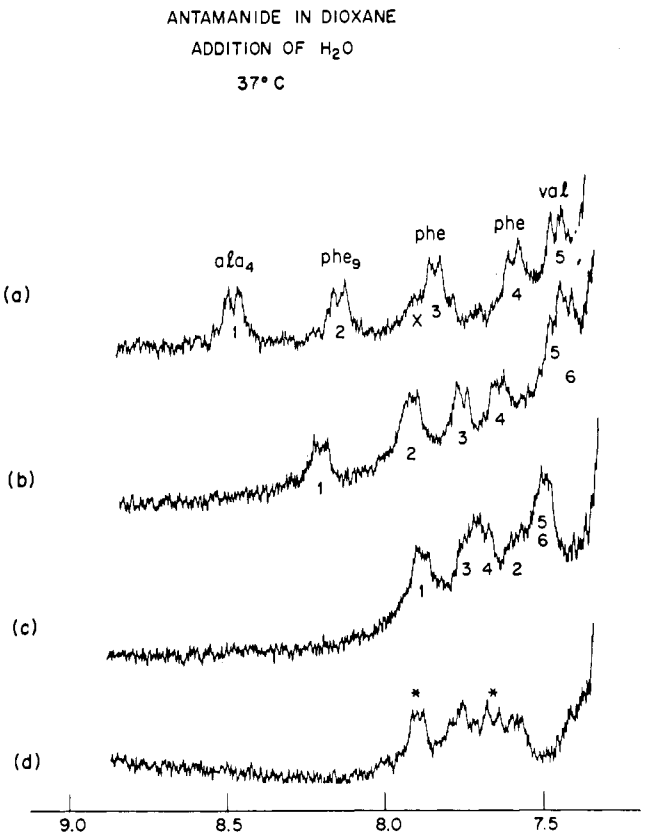

FIGURE 9: Chemical-shift changes for the peptide N protons of antamanide in dioxane (spectrum a) on addition of H_2O (spectra b, c, and d). Further addition of H_2O had no effect on spectrum d.

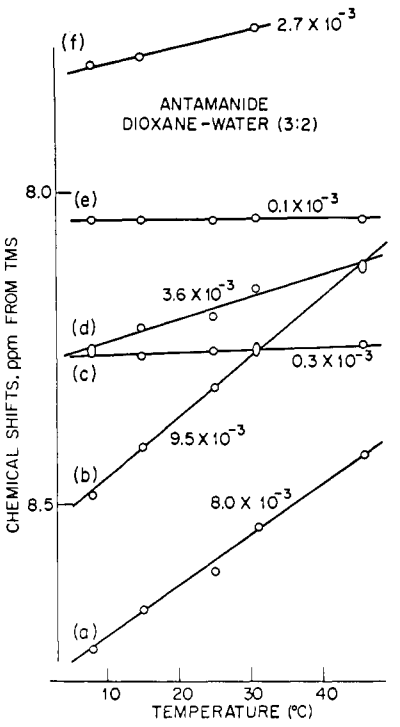

FIGURE 10: The temperature coefficients for the peptide N protons of antamanide in dioxane–water (3:2).

gest that the peptide protons of Val_1 and Phe_6 form short coplanar intramolecular hydrogen bonds, those of Ala_4 and Phe_9 are exposed to solvent, while the peptide N protons of Phe_5 and Phe_{10} form weak intramolecular hydrogen bonds and/or are solvent shielded. Coupling constant and chemical-shift changes were observed on complexation permitting an identification of those residues undergoing conformational change. Sodium exchange between antamanide and its complex manifested itself in line-width changes at sodium/antamanide of <1, but separate narrow resonances for the decapeptide and its complex were not observed simultaneously. This suggests that cis–trans peptide bond isomerization did not take place on complexation. An analysis of the C^{β} and C^{γ} carbon chemical shifts suggests that the complex contains two cis and two trans X-Pro peptide bonds.

Low-energy conformations for the complex containing a cavity for metal ion binding were generated with all-trans peptide bonds (*trans*-complex), cis peptide bonds at Val_1-Pro_2 and Phe_6-Pro_7 (1,6-*cis*-complex), and cis peptide bonds at Pro_2-Pro_3 and Pro_7-Pro_8 (2,7-*cis*-complex). These conformations were constructed from molecular model building and exhibited φ values consistent with $J_{H^N H^\alpha}$ coupling constants, ψ values in the range 280–340 for an X residue in an X-Pro sequence, intramolecular hydrogen bonds suggested from temperature coefficient and exchange data, and rotational angles consistent with low-energy regions of the conformational energy maps. These conformations are defined in terms of φ, ψ, and ω rotation angles and photographs of CPK models presented. The experimental evidence appears to be more consistent with conformation 1,6-*cis*-complex, containing cis peptide bonds at Val_1-Pro_2 and Phe_6-Pro_7, for antamanide–Na in solution. A conformation for the complex suggested by Ivanov *et al.* (1971) is reviewed.

Antamanide Conformation in Aqueous Media. The solvent-dependent conformations of antamanide in nonaqueous solution were outlined in the previous article (Patel, 1973). The conformation in weak hydrogen-bond acceptor nonaqueous media (designated I) contains all intramolecularly hydrogen-bonded peptide protons. This conformation occurs in rapid equilibrium with a conformation with all peptide protons exposed to solvent (designated II) in strong hydrogen-bond acceptor nonaqueous media.

From ORD studies (Ivanov *et al.*, 1969) and CD studies (Faulstich *et al.*, 1972) it was shown that antamanide in organic solvents undergoes a large conformational change on addition of water. Further, the CD spectra of antamanide in aqueous media and antamanide–Na in organic solvents are strikingly similar over the range 200–260 nm suggesting a similar conformation for the polypeptide (Faulstich *et al.*, 1972).

Antamanide is insoluble in water and therefore has been investigated in dioxane–water mixtures. The H^{α} region cannot be observed because of the strong H_2O resonance at 4.5 ppm and this prevents spectral assignments from decoupling studies. Since the antamanide spectral assignments were known in dioxane, an attempt was made to follow the peptide NH resonances on gradual addition of H_2O.

The peptide N proton region of the nmr spectra of antamanide in dioxane is shown in Figure 9a and in dioxane–water, under conditions where further water addition had no effect (in Figure 9d). At intermediate water concentrations, Figures 9b and 9c, average sharp resonances were observed, suggesting the absence of cis–trans peptide bond isomerization on addition of water to antamanide in nonaqueous solvents. Attempts to identify the peptide N protons for antamanide in dioxane–water, Figure 9d, were unsuccessful, since the crossover of resonances on addition of water to antamanide in dioxane could not be sorted out.

The temperature coefficients for antamanide in dioxane–water (3:2) are outlined in Figure 10. Two peptide NH resonances exhibit small temperature coefficients of 0.1×10^{-3} and 0.3×10^{-3} ppm/°C suggesting that these protons participate in short coplanar intramolecular hydrogen bonds. Two peptide NH resonances exhibit large temperature coefficients of 9.5×10^{-3} and 8.0×10^{-3} ppm suggesting that these protons are exposed to solvent. The remaining two peptide NH resonances exhibit intermediate temperature coefficients of 2.7×10^{-3} and 3.6×10^{-3} ppm/°C and are suggested to either participate in weaker intramolecular hydrogen bonds and/or are solvent shielded. These temperature coefficients for the six peptide protons of antamanide in dioxane–water (3:2) are similar to the values observed for antamanide–Na in organic solvents.

It has not been possible to assign these temperature coefficients to specific residues in antamanide nor has it been possible to measure the $J_{H^N H^\alpha}$ coupling constants accurately. Attempts to generate a conformation for antamanide in aqueous media must await accumulation of additional nmr data.

In summary, this investigation reaches two conclusions toward the prediction of the conformation of antamanide in aqueous solution. Since there is not cis–trans peptide bond isomerization on addition of water to antamanide in nonaqueous solvent dioxane, the conformation of the cyclic decapeptide in aqueous media must contain two cis X-Pro peptide bonds. The temperature coefficients for the peptide NH protons for antamanide in aqueous media are similar to those observed for the antamanide–Na complex, suggesting a similarity in conformation as suggested earlier by Faulstich *et al.* (1972).

Acknowledgments

Antamanide was generously provided by Professor Th. Wieland. Discussions with Professor Th. Wieland and Professor Yu. Ovchinnikov were most helpful.

References

Barfield, M., and Karplus, M. (1969), *J. Amer. Chem. Soc. 91*, 1.

Brant, D. A., and Flory, P. J. (1965), *J. Amer. Chem. Soc. 87*, 2791.

Bystrov, V. F., Portnova, S. L., Tsetlin, V. I., Ivanov, V. T., and Ovchinnikov, Yu. A. (1969), *Tetrahedron 25*, 493.

Cowan, P. M., and McGavin, J. (1955), *Nature (London) 716*, 501.

Crippen, G. M., and Scheraga, H. A. (1969), *Proc. Nat. Acad. Sci. U. S. 64*, 42.

Deber, C. M., Torchia, D. A., and Blout, E. R. (1971), *J. Amer. Chem. Soc. 93*, 4893.

Deber, C. M., Torchia, D. A., Wong, S. C. K., and Blout, E. R. (1972), *Proc. Nat. Acad. Sci. U. S. 69*, 1825.

DeSantis, P., Giglio, E., Liquori, A. M., and Ripamonti, A. (1965), *Nature (London) 206*, 456.

Edsall, J. T., Flory, P. J., Kendrew, J. C., Liquori, A. M., Nemethy, G., Ramachandran, G. N., and Scheraga, H. A. (1966), *Biopolymers 4*, 121.

Faulstich, H., Burgermeister, W., and Wieland, Th. (1972), *Biochem. Biophys. Res. Commun. 47*, 975.

Go, N., and Scheraga, H. A. (1970), *Macromolecules 3*, 188.

Ivanov, V. T., Miroshnikov, A. I., Abdullaev, N. D., Senyavina, L. B., Arkhipova, S. F., Uvarova, N. N., Khalilulina, K. Kh., Bystrov, V. F., and Ovchinnikov, Yu. A. (1971), *Biochem. Biophys. Res. Commun. 42*, 654.

Kopple, K. D. (1971), *Biopolymers 10*, 1139.

Leung, Y. C., and Marsh, R. E. (1958), *Acta Crystallogr. 11*, 17.

Patel, D. J. (1973), *Biochemistry 12*, 667.

Pullman, B., and Maigret, B. (1972), Conference on Conformation of Biological Molecules and Polymers, Jerusalem, Israel, April 3–9.

Ramachandran, G. N., Chandrasekaran, R., and Kopple, K. D. (1970), Second American Peptide Symposium, Cleveland, Ohio, August 17–19, paper No. 28.

Ramakrishnan, C., and Ramachandran, G. N. (1965), *J. Biophys. 5*, 909.

Sasisekharan, V. (1959), *Acta Crystallogr. 12*, 897.

Schimmel, P. R., and Flory, P. J. (1967), *Proc. Nat. Acad. Sci. U. S. 58*, 52.

Schimmel, P. R., and Flory, P. J. (1968), *J. Mol. Biol. 34*, 105.

Shchori, E., Jagur-Grodzinski, J., Luz, Z., and Shporer, M. (1971), *J. Amer. Chem. Soc. 93*, 7133.

Stern, A., Gibbons, W. A., and Craig, L. C. (1968), *Proc. Nat. Acad. Sci. U. S. 61*, 735.

Sternlicht, H., and Zuckerman, D. (1972), *Rev. Sci. Instrum. 43*, 525.

Tonelli, A. E. (1973), *Biochemistry 12*, 689.

Tonelli, A. E., Patel, D. J., Goodman, M., Naider, F., Faulstich, H., and Wieland, Th. (1971), *Biochemistry 10*, 3211.

Torchia, D. A. (1971), *Macromolecules 4*, 440.

Torchia, D. A. (1972), *Biochemistry 11*, 1462.

Torchia, D. A., DiCorato, A., Wong, S. C. K., Deber, C. M., and Blout, E. R. (1972a), *J. Amer. Chem. Soc. 94*, 609.

Torchia, D. A., Wong, S. C. K., Deber, C. M., and Blout, E. R. (1972b), *J. Amer. Chem. Soc. 94*, 616.

Urry, D. W., and Ohnishi, M. (1972), Spectroscopic Approaches to Biomolecular Conformation, Urry, D. W., Ed., Chicago, Ill., American Medical Association Press, p 263.

Venkatachalam, C. M. (1968), *Biopolymers 6*, 1425.

Wieland, Th., Faulstich, H., and Burgermeister, W. (1972), *Biochem. Biophys. Res. Commun. 47*, 984.

Wong, K. H., Konizer, G., and Smid, J. (1970), *J. Amer. Chem. Soc. 92*, 666.